A Novel Ferroptosis-related Gene Signature for Prognosis Prediction in Glioma

Tian Lan
Wuhan University Second Clinical College: Wuhan University Zhongnan Hospital https://orcid.org/0000-0002-4020-9824
Die Wu
Wuhan University Second Clinical College: Wuhan University Zhongnan Hospital
Wei Quan
Wuhan University Second Clinical College: Wuhan University Zhongnan Hospital
Donghu Yu
Wuhan University Second Clinical College: Wuhan University Zhongnan Hospital
Sheng Li
Wuhan University Second Clinical Hospital: Wuhan University Zhongnan Hospital
Jie Yao
Human Genetic Resources Preservation Center of Hubei Province
Zhi-Qiang Li (lizhiqiang@whu.edu.cn)
Zhongnan Hospital of Wuhan University https://orcid.org/0000-0002-4148-780X

Primary research

Keywords: ferroptosis, glioma, gene signature, prognosis

Posted Date: September 22nd, 2021

DOI: https://doi.org/10.21203/rs.3.rs-829477/v1

Abstract

Background: Glioma is a fatal brain tumor characterized by invasive nature, rapidly proliferation and tumor recurrence. Despite aggressive surgical resection followed by concurrent radiotherapy and chemotherapy, the overall survival (OS) of Glioma patients remains poor. Ferroptosis is a unique modality to regulate programmed cell death and associated with multiple steps of tumorigenesis of a variety of tumors.

Methods: In this study, ferroptosis-related genes model was identified by differential analysis and Cox regression analysis. GO, KEGG and GSVA analysis were used to detect the potential biological functions and signaling pathway. The infiltration of immune cells was quantified by Cibersort.

Results: The patients' samples are stratified into two risk groups based on 4-gene signature. High-risk group has poorer overall survival. The results of functional analysis indicated that the extracellular matrix-related biologic functions and pathways were enriched in high-risk group, and that the infiltration of immunocytes is different in two groups.

Conclusion: In summary, a novel ferroptosis-related gene signature can be used for prognostic prediction in glioma. The filtered genes related to ferroptosis in clinical could be a potential extra method to assess glioma patients' prognosis and therapeutic.

Background

Glioma is the most common primary malignant brain tumor, representing 81% of all malignant brain tumors[1]. According to World Health Organization, glioma is graded into 4 levels (I ~ IV). The 10-year survival rate of patients with low-grade glioma (WHO grade II ~ III glioma) is 47% with a median survival time of 11.6 years[2]. Glioblastoma (WHO grade IV glioma) patients who received post-operative radiation and concurrent temozolomide, have a median survival of 14.6 months[3]. Since patients with gliomas have such a poor prognosis, and currently the predictive prognosis ability of clinical testing indicators is weak and deficient, additional predictive models as novel biomarkers are needed to fill the vacancy. 2007 classification relied on histological analysis while 2016 classification incorporated molecular markers[4, 5]. Some molecular markers of glioma: deletion of short arm Ch.1 and long arm of Ch.19 (1p/19q)[6], methylation of O6-methylguanine-DNA methyltransferase (MGMT)[7], mutation of isocitrate dehydrogenase 1 (IDH1)[8] were involved, but numerous clinical trails of glioma therapies that targeting these biomakers failed to demonstrate a robust therapeutic effect. Therefore, additional indicators need to be supplemented to comprehensively predict the prognosis of glioma patients.

Ferroptosis, characterized by iron-dependent lipid peroxidation, is a newly non-apoptotic form of cell death that is widely implicated in human pathological conditions[9]. It has been reported that ferroptosis plays a vital role in the pathogenesis of a growing list of disease, such as cancer, neurological disorders, including neurodegenerative diseases and brain damage, as a way to promote cell death[10–14], liver and lung fibrosis[15, 16] and autoimmune disease[17, 18]. Furthermore, some ferroptotic regulatory genes, such as GPX4[19], ACSL4[20], FANCD2[21], SLC7A11[22], have been reported to be closely related to tumor proliferation and migration. As such, the development of ferroptosis induction-based cancer therapies is being actively explored, such as hepatocellular carcinoma[23], pancreatic cancer[24], gastric cancer[25] and non-small cell lung carcinoma[26]. Thus, modulating ferroptosis activities could hold promise for therapeutic development against malignant diseases.

Given this, our study aimed to screen out genes associated ferroptosis with glioma from multiple gene expression datasets, to explore novel biomakers that can help to supplementally and comprehensively predict the prognosis of glioma. Furthermore, we also explore ferroptosis-related genes and potential molecular mechanism of prognostic

differences in glioma. Our study suggest that ferroptosis-related genes may be potential prognostic markers and therapeutic targets for glioma.

Methods

Datasets and experimental process

All datasets we used are available to public. We selected TCGA dataset (Genotype-Tissue Expression (GTEx) dataset as control dataset) as a derivation cohort. CGGA , Gravendeel and REMBRANDT datasets were chosen as validation cohorts. The RNA-seq data, clinical information and molecular information were downloaded from UCSC-XENA (http://xena.ucsc.edu), CGGA (http://www.cgga.org.cn) and GlioVis (http://gliov is.bioin fo.cnio. es/). 687 patients from TCGA (5 normal samples and 2 samples without clinical messages were excluded), 105 controls from GTEx, 693 patients from CGGA, 276 patients from Gravendeel (8 normal samples were excluded) and 383 patients from REMBRANDT (92 sample with normal or missing histological classification were excluded) were finally enrolled in this study. The details of clinical and molecular information of those samples are shown in Table 1. The process of the study is shown in Figure 1.

DEGs of GBM and LGG from TCGA-GTEx

The package “edgeR”[27, 28] and “limma”[29] in R were used to identify differentially expressed genes (DEGs) between glioma (171 Glioblastoma multiforme (GBM), 523 Brain Lower Grade Glioma (LGG) from TCGA) and normal brain tissues (105 Normal samples from GTEx). Adjusted P values below 0.05 (Adj. $P < 0.05$) and absolute value of fold change ($\log_2$FC) above 1 ($|\log_2 FC > 1|$) were considered statistically significant.

The construction and validation of gene-associated prognostic model

Univariate and multivariate Cox regression analyses were applied to analyze the relationships between patient’ overall survival (OS) and the expression level of each ferroptosis-related genes. Under threshold of $p<0.01$ in the univariate Cox regression analysis, the gene was selected significant. We finally selected 4 genes by using the multivariate Cox regression to assess the contribution of gene as independent prognostic factor for patient survival and created a model. A 4-gene signature model of risk score was established based on a linear combination of the regression coefficient derived from the multivariate Cox regression model (coefficient) multiplied by its expression level. The prognosis index (PI) = (coefficient*expression level of FANCD2) + (coefficient*expression level of IGFBP3) + (coefficient*expression level of LPCAT3) + (coefficient*expression level of HMOX1). Cut-off value is the limit of the maximum value obtained by the Yoden index from receiver operating characteristic (ROC) curve by "survivalROC"[30] package. According to the cut-off value, the patients were grouped under low-risk and high-risk. The "survminer" (https://cran.r-project.org/web/packages/survminer/survminer.pdf) package in R was utilized to conduct Kaplan-Meier (KM) survival curves for the samples with low- and high-risk group. Univariate and multivariate Cox regression analyses were employed to certify whether the predictive power of prognostic model could be independent of other clinical variables (containing Age, Gender, tumor Grade, IDH1 Status and histology) for glioma patients. The hazard ratio (HR) with 95% confidence intervals (CI) were calculated.

Functional Enrichment Analysis

Gene ontology (GO) and Kyoto Encyclopedia of Genes and Genomes (KEGG) are used to detect the potential biological functions and signaling pathway by the “clusterProfiler”[31] package. GeneMANIA (http://www.genemania.org) is used to conduct the gene-gene interaction network and potential pathways based on the DEGs between high-risk and low-risk group. Gene Set Variation Analysis (GSVA)[32] is used to estimate variation of gene set enrichment in four datasets, thereby allowing the evaluation of pathway enrichment for each sample.

Immune infiltration

To explore the immune infiltration in high risk and low risk group related to ferroptosis in glioma, “CIBERSORT”[33] package was used to assess the proportions of 22 immune cell subtypes based on expression file. The perm was set at 1000. Samples with $P < 0.05$ in CIBERSORT analysis result were used in further analysis. Mann-Whitney U test was used to compare differences in immune cell subtypes in the high-risk score and low-risk score groups.

Statistical Analysis

R software (version 4.0.2) and SPSS software (version 23.0) were used to complete all the statistical analysis. The log-rank test, and the differences between categorical variables were compared by using the Chi-square test. Independent prognostic factors were assessed by univariate and multivariate Cox regression. GO and KEGG analyses were calculated by Mann-Whitney U test with P values adjusted by the BH method. $P < 0.05$ was considered statistically significant.

Results

Identification of 4 ferroptosis-related candidate genes in Glioma Patients

A total of 55 ferroptosis-related genes were inclued from previous studies[16, 34-42] (Supplement table 1). 20 ferroptosis-related genes (20/55, 36.4%, TP53, SLC1A5, CD44, HSPA5, PROCR, SLC40A1, LPCAT3, HMOX1, PANX1, IGFBP7, ALOX5AP, FANCD2, STEAP3, SERPINE1, CDKN1A, IGFBP3, BDNF, HIC1, MT1G, CHAC1) were found in 4352 DEGs from TCGA-GTEx datasets. (Figure 2A and Table 2). Ferroptosis-related prognostic DEGs (FANCD2, TP53, IGFBP3, LPCAT3, SLC40A1, HMOX1) was filtrated through the univariate Cox regression analysis (Figure 2B). TP53 and SLC40A1 were not significant to be excluded by multivariate Cox regression analysis (Figure 2C). The co-linearity was checked between these genes to measure the connection among them and the result showed that the genes were independent of each other and the construction of model is available (Figure 2D). Finally, 4 genes as prognostic model factors were determined (FANCD2, IGFBP3, LPCAT3, HMOX1, Figure 2E).

Prognostic model construction in TCGA cohort

The risk score was calculated according to the expression of these ferroptosis-related genes in TCGA dataset, as formula: (0.504*expression level of FANCD2 + 0.264*expression level of HMOX1 + 0.235*expression level of IGFBP3 + 0.267*expression level of LPCAT3) (Supplementary table 2). Patients were ranked by the score, and they were stratified into a low-risk group (n=436) and a high-risk group (n=251) based on the optimal cut-off expression value. Patients in the low-risk group had prolonged OS than high-risk group (Figures 3A-C). The predictive performance of the risk model for OS was estimated by time-dependent ROC curves. The results showed that the area under the curve (AUC) reached 0.843 at 1 year, 0.846 at 2 years, and 0.849 at 3 years respectively (Figure 3D).

External validation of 4-gene prognosis model

From the analysis above, the model was able to effectively predict glioma patients' prognosis in TCGA dataset. Subsequently, CGGA, Gravendeel and REMBRANDT datasets were performed to verify the efficacy and availability of the model. The patients in CGGA, Gravendeel and REMBRANDT datasets were also grouped into low-risk and high-risk respectively. The results in three datasets showed that high-risk group had a markedly poor prognosis than low-risk group (Figures 3A-C), suggesting that the 4-gene signature model can greatly predict the prognosis of patients. Time-dependent ROC curves were plotted to illustrate the sensitivity and specificity of the model. The 1-, 3- and 5-year AUC values of CGGA are 0.654, 0.718 and 0.738; of Gravendeel are 0.741, 0.729 and 0.770 respectively; and the 1-, 2-, and 3-year AUC values of REMBRANDT are 0.649, 0.744 and 0.740 (Figure 3D). According to the results of AUC curve, the prognostic model was significant.

Clinical characteristics of the patients based on risk score

The heatmaps (Figure 4A) showing the differential expression of the 4 selected genes, and baseline characteristics of the patients in different risk groups (Table 3) suggested that clinical and molecular features, such as WHO grade, age, classical subtypes, mesenchymal subtypes, and IDH wild types were enriched in high-risk group. Furthermore, with an increase in glioma grade, the risk score increased. The highest increase in risk score was found in the WHO grade IV patients, whereas the lowest increase in risk score was observed in the WHO grade II patients in the TCGA, CGGA, Gravendeel and REMBRANDT datasets (Figure 4B). Meanwhile, Kaplan-Meier plots of overall survival based on different clinical characters presented apparent differences between the high-risk group and low risk group for survival (Figures 5A-H). The survival-predictor scores from these models were highly predictive of survival in datasets ($p < 0.001$). The 4-gene mod was able to distinguish patients with obviously distinct outcomes across subsets, demonstrating the risk score based on four gene was greater prognostic power as compared with only used of clinical subgroups (WHO grade, IDH1, MGMT, 1p/19q).

Independent Prognostic Value of the 4-gene Signature

The independence of the clinical prognostic significance of the signature in glioma was verified. The risk score was significantly associated with OS in univariate Cox regression analysis in TCGA, CGGA, Gravendeel and REMBRANDT datasets, and the Hazard ratio (HR) of four datasets were: 9.57, 3.64, 2.80, 3.18 (95%CI, Under threshold of $p<0.001$) respectively (Table 4). Multivariate regression analysis still showed a significant correlation of the risk score with OS after adjusting for other clinical factors. The HR of multivariate analysis in four databases are 2.50, 1.87, 1.80, 1.87 (95%CI, Under threshold of $p<0.001$) (Figure 6). Consequently 4-gene signature model can be determined to be an independent prognostic factor of survival.

The Clinical Predictive Performance of the Nomogram

Based on the four ferroptosis-related gene signature (risk score) and clinical factor, a nomogram to predict patients' prognosis in the TCGA database was created (Figure 7A). In the study, we used a bootstrap method to verify the developed nomogram with the C-index of 0.869（95%CI), which suggested that the predictive model had good predictive performance. Furthermore, the calibration curves in 1-, 2-, 3-year survival of patients also showed good consistency compared with the ideal model, further indicating that the nomogram was stable in predicting the prognosis of glioma patients (Figures 7B-D). This suggests that basing therapy strategy on our nomogram will improve clinical outcome (Figure 7E).

Functional Annotation of the 4-gene Signature

To clarify the potential functional characteristics associated with risk score, the DEGs between the low-risk and high-risk groups were used to perform GO enrichment and KEGG pathway analyses. The results of GO enrichment were concentrated in three areas: binding with skeleton-associated, changing of receptor channel and extracellular matrix constituent, extracellular matrix could be a pro-ferroptosis stress, which may mediate cell adhesion, vesicular bodies and exosomes resulted in poor prognosis for high-risk groups. The results indicated that the biological processes associated with extracellular matrix and cell adhesion were enriched in high-risk group (*P*. adjust < 0.05, Figure 8A). KEGG pathway analysis also showed that the ECM−receptor interaction pathway and the Focal adhesion pathway were significantly enriched in high-risk group (*P*. adjust < 0.05, Figure 8B). Meanwhile, the results of GeneMANIA also confirmed that the high-risk group was obviously gathered in the structure, organization and disassembly of extracellular matrix (Figure 8C). These enriched biologic functions thus provided a deeper understanding of the patients' poor prognosis.

Relationship between ferroptosis and Immune infiltration

Analysis of hallmark pathway gene signatures indicated that signaling pathways gathering at various biological progress were significantly different between high- and low-risk patients (Figure 9A-D). Different database has also different enrich result of signaling pathways. Immune related signal pathways are enriched in four different databases. (Figure 9E-F) (Interferon Gamma Respnse, TNFA Signaling Via NFκB and Interferon Alpha response 3/7). Recent study has been reported that due to the multifaceted nature and the involvement of numerous metabolic pathways directly impinging on ferroptosis, it is highly likely that certain key nodes of the ferroptosis process are targeted by the immune system[43]. To further explore the correlation between the model and immune status, enrichment scores of the diverse immune cell subpopulations in TCGA and CGGA were quantified by Cibersort. Various immune cells (CD4+T cell, CD8+T cell, Tregs, monocytes, macrophages M0/M2, NK cells) were obviously different between the high risk and low risk (Figure 9G-H). The immune infiltrations of the two databases perfectly shows that the four ferroptosis-gene model are closely relevant to the immune.

Discussion

Glioma is the main malignant tumor in primary brain tumors. At present, the prognostic prognosis signature in brain tumors include IDH1, MGMT, etc. subtype classification is helpful to better predict the survival time of subgroups based on the biological detection indexes[44]. The combination of IDH1, MGMT and other biological indicators helped to easily achieve this expectation. Otherwise, the molecular pathway mechanism of glioma prognosis in other fields needed to be expanded. Ferroptosis is a regulatory form of non-apoptotic cell death, which is characterized by the accumulation of iron dependent lethal lipid reactive oxygen species (ROS). There had been a break-through in tumor and ferroptosis. Some studies had shown that ferroptosis and glioma was closely correlative, but there were few data analysis studies to clearly explain the relationship between iron death and glioma prognosis. A prognosis prediction model was created by using four public databases based on ferroptosis-related genes to further explore the prognosis correlated ferroptosis to glioma as well as the potential biological relevance.

It had been reported that the ferroptosis-related genes had diverse functions influencing tumor's progress, such as migration, invasion, angiogenesis and immune infiltration. Based on GO and KEGG function analysis, cell adhesion, extracellular matrix, exosomes were obviously enriched, which was correlated with immune microenvironment in glioma reported by previous studies. gliomas were characterized by profound immunosuppression mediated by secreted (TGF-β, IL-10) and cell surface (CD95L, PD-L1) immunosuppressive factors, by infiltration of immune inhibitory cells in the tumor microenvironment and by anatomical peculiarities of the brain[45]. Immune infiltration in our study also presented that

ferroptosis prognosis genes were closely related to the immune. Interestingly, previous studies showed that HMOX1 and IGFBP-3 were significantly associated with immune. The enzyme heme oxygenase-1 (HOMX1) was part of an endogenous defense system implicated in the homeostatic response, data were available from a wide spectrum of physiopathologic conditions that link HOMX1 to modulation of angiogenesis and the immune function. The immunodulatory function of HOMX1 is well documented and its immunosuppressive role is widely accepted[46]. It had reported that Hemin treatment resulted in enhanced CTL effector function both in normal and tumor microenvironments. Insulin-like growth factor 1 (IGF-I) and IGF-II were members of the insulin superfamily of growth-promoting peptides and were among the most abundant and ubiquitous polypeptide growth factors[47]. The IGFBPs were secreted proteins that were also found intracellularly and that interact with many ligands other than the IGFs. IGFBP-3 was determined to activate the type 1 TGFβ receptor and its downstream effectors SMAD2 and SMAD3 to inhibit breast cancer cell growth[48]. Phospholipid-remodeling enzyme, lysophosphatidylcholine acyltransferase 3 (Lpcat3), as a critical determinant of membrane phospholipid composition, was important drivers of ferroptosis. Loss of Lpcat3 or activation of SREBP-2 in Apcmin mice markedly promote intestinal tumor formation[49]. In other word, Lipid metabolism marked as LPCAT3 might be potential correlated to immune as HMOX1 and IGFBP3.but it needed to be verified by further studies. Moreover, IGFBP-3 had been acting as a marker of prognosis in various tumor.

Four genes prognosis model with FANCD2, HMOX1, LPCAT3 and IGFBP3 were identified in 4 datasets. We attested that the 4-gene signature is a clinical promising biomarker, which could classify glioma patients into subgroups. Our function analysis presented that ferroptosis was closely associated with the immune and further predicted the existence of potential relationship between the lipid metabolism and the immune in glioma. Previous studies showed that blocking key enzymes, such as fatty acid synthase (FASN), which is required for the synthesis of palmitate from acetyl-CoA and malonyl-CoA48, and ELOVL fatty acid elongase 2 (ELOVL2), which catalyses the elongation of fatty acids, suppressed glioma tumor growth in GBM xenograft models, indicating that fatty acids are required for glioma growth and survival[50, 51]. But it’s needed to further understand the mechanisms of ferroptosis as well as its effect to glioma.

Conclusions

In conclusion, a novel ferroptosis-related gene signature, which could classify glioma patients into subgroups, can be used for prognostic prediction in glioma. The 4-gene model in clinical could be a potential extra method to assess glioma patients’ prognosis and therapeutic.

Abbreviations

OS: overall survival;

IDH1: isocitrate dehydrogenase 1;

MGMT: methylation of O6-methylguanine-DNA methyltransferase;

1p/19q: deletion of short arm Ch.1 and long arm of Ch.19;

TCGA: The Cancer Genome Atlas dataset;

GTEx: Genotype-Tissue Expression;

CGGA: the Chinese Glioma Genome Atlas dataset;

REMBRANDT: the Repository of Molecular Brain Neoplasia Data dataset;

DEGs: differentially expressed genes;

GBM: Glioblastoma multiforme;

LGG: Brain Lower Grade Glioma;

Log2FC: absolute value of fold change;

ROC: receiver operating characteristic curve;

KM: Kaplan-Meier survival curves;

HR: The hazard ratio;

CI: confidence intervals;

GO: Gene ontology;

KEGG: Kyoto Encyclopedia of Genes and Genomes;

GSVA: Gene Set Variation Analysis;

AUC: Area Under Curve;

ECM: extracellular matrix;

TNFA: tumor necrosis factor-α;

ROS: reactive oxygen species;

TGF-β: transforming growth factor-β;

IL: Interleukin;

CD: Cluster of Differentiation;

PD-L1: programmed cell death-Ligand 1;

IGF-I: Insulin-like growth factor 1;

SREBP-2: Sterol-regulatory element binding proteins 2;

FASN: fatty acid synthase;

ELOVL: fatty acid elongase.

Declarations

Acknowledgements

Not applicable

Authors’ contributions

LT and WD: designed the study, reviewed relevant literature and drafted the manuscript. QW and YDH conducted all statistical analyses. LT, WD and LS: revise the manuscript. All authors read and approved the final manuscript.

Funding

This work was funded in part by the Translational Medicine Fund of the Zhongnan Hospital of Wuhan University (No. ZLYNXM202011, ZNLH201901), and the National Health Commission of China (2018ZX-07S-011).

Availability of data and materials

The data sets used and/or analyzed during the current study are available from the corresponding author on reasonable request.

Ethics approval and consent to participate

Not applicable

Consent for publication

We assure that the material is original and it has not been published elsewhere yet.

Competing interest

The authors declare no conflict of interest.

References

1. Ostrom QT, Bauchet L, Davis FG, Deltour I, Fisher JL, Langer CE, Pekmezci M, Schwartzbaum JA, Turner MC, Walsh KM, et al. The epidemiology of glioma in adults: a "state of the science" review. Neurooncology. 2014;16(7):896–913.
2. Smoll NR, Gautschi OP, Schatlo B, Schaller K, Weber DC. Relative survival of patients with supratentorial low-grade gliomas. Neuro Oncol. 2012;14(8):1062–9.
3. Stupp R, Mason WP, van den Bent MJ, Weller M, Fisher B, Taphoorn MJ, Belanger K, Brandes AA, Marosi C, Bogdahn U, et al. Radiotherapy plus concomitant and adjuvant temozolomide for glioblastoma. N Engl J Med. 2005;352(10):987–96.
4. Louis DN, Ohgaki H, Wiestler OD, Cavenee WK, Burger PC, Jouvet A, Scheithauer BW, Kleihues P. The 2007 WHO classification of tumours of the central nervous system. Acta Neuropathol. 2007;114(2):97–109.
5. Louis DN, Perry A, Reifenberger G, von Deimling A, Figarella-Branger D, Cavenee WK, Ohgaki H, Wiestler OD, Kleihues P, Ellison DW. The 2016 World Health Organization Classification of Tumors of the Central Nervous System: a summary. Acta Neuropathol. 2016;131(6):803–20.
6. Cairncross G, Jenkins R. Gliomas with 1p/19q codeletion: a.k.a. oligodendroglioma. Cancer J. 2008;14(6):352–7.
7. Esteller M, Garcia-Foncillas J, Andion E, Goodman SN, Hidalgo OF, Vanaclocha V, Baylin SB, Herman JG. Inactivation of the DNA-repair gene MGMT and the clinical response of gliomas to alkylating agents. N Engl J Med. 2000;343(19):1350–4.

8. Yan H, Parsons DW, Jin G, McLendon R, Rasheed BA, Yuan W, Kos I, Batinic-Haberle I, Jones S, Riggins GJ, et al. IDH1 and IDH2 mutations in gliomas. N Engl J Med. 2009;360(8):765–73.
9. Hirschhorn T, Stockwell BR. The development of the concept of ferroptosis. Free Radic Biol Med. 2019;133:130–43.
10. Alim I, Caulfield JT, Chen Y, Swarup V, Geschwind DH, Ivanova E, Seravalli J, Ai Y, Sansing LH, Ste Marie EJ, et al. Selenium Drives a Transcriptional Adaptive Program to Block Ferroptosis and Treat Stroke. Cell. 2019;177(5):1262–79.e1225.
11. Hambright WS, Fonseca RS, Chen L, Na R, Ran Q. Ablation of ferroptosis regulator glutathione peroxidase 4 in forebrain neurons promotes cognitive impairment and neurodegeneration. Redox Biol. 2017;12:8–17.
12. Tuo QZ, Lei P, Jackman KA, Li XL, Xiong H, Li XL, Liuyang ZY, Roisman L, Zhang ST, Ayton S, et al. Tau-mediated iron export prevents ferroptotic damage after ischemic stroke. Mol Psychiatry. 2017;22(11):1520–30.
13. Wu JR, Tuo QZ, Lei P. Ferroptosis, a Recent Defined Form of Critical Cell Death in Neurological Disorders. J Mol Neurosci. 2018;66(2):197–206.
14. Zille M, Karuppagounder SS, Chen Y, Gough PJ, Bertin J, Finger J, Milner TA, Jonas EA, Ratan RR. Neuronal Death After Hemorrhagic Stroke In Vitro and In Vivo Shares Features of Ferroptosis and Necroptosis. Stroke. 2017;48(4):1033–43.
15. Yu Y, Jiang L, Wang H, Shen Z, Cheng Q, Zhang P, Wang J, Wu Q, Fang X, Duan L, et al. Hepatic transferrin plays a role in systemic iron homeostasis and liver ferroptosis. Blood. 2020;136(6):726–39.
16. Zhang Z, Yao Z, Wang L, Ding H, Shao J, Chen A, Zhang F, Zheng S. Activation of ferritinophagy is required for the RNA-binding protein ELAVL1/HuR to regulate ferroptosis in hepatic stellate cells. Autophagy. 2018;14(12):2083–103.
17. Hu CL, Nydes M, Shanley KL, Morales Pantoja IE, Howard TA, Bizzozero OA. Reduced expression of the ferroptosis inhibitor glutathione peroxidase-4 in multiple sclerosis and experimental autoimmune encephalomyelitis. J Neurochem. 2019;148(3):426–39.
18. Kim EH, Wong SW, Martinez J. Programmed Necrosis and Disease:We interrupt your regular programming to bring you necroinflammation. Cell Death Differ. 2019;26(1):25–40.
19. Seibt TM, Proneth B, Conrad M. Role of GPX4 in ferroptosis and its pharmacological implication. Free Radic Biol Med. 2019;133:144–52.
20. Cheng J, Fan YQ, Liu BH, Zhou H, Wang JM, Chen QX. ACSL4 suppresses glioma cells proliferation via activating ferroptosis. Oncol Rep. 2020;43(1):147–58.
21. Song X, Xie Y, Kang R, Hou W, Sun X, Epperly MW, Greenberger JS, Tang D. FANCD2 protects against bone marrow injury from ferroptosis. Biochem Biophys Res Commun. 2016;480(3):443–9.
22. Lang X, Green MD, Wang W, Yu J, Choi JE, Jiang L, Liao P, Zhou J, Zhang Q, Dow A, et al: **Radiotherapy and Immunotherapy Promote Tumoral Lipid Oxidation and Ferroptosis via Synergistic Repression of SLC7A11**. *Cancer Discov* 2019, **9**(12):1673–1685.
23. Nie J, Lin B, Zhou M, Wu L, Zheng T. Role of ferroptosis in hepatocellular carcinoma. J Cancer Res Clin Oncol. 2018;144(12):2329–37.
24. Song Z, Xiang X, Li J, Deng J, Fang Z, Zhang L, Xiong J. Ruscogenin induces ferroptosis in pancreatic cancer cells. Oncol Rep. 2020;43(2):516–24.
25. Wang C, Shi M, Ji J, Cai Q, Zhao Q, Jiang J, Liu J, Zhang H, Zhu Z, Zhang J. Stearoyl-CoA desaturase 1 (SCD1) facilitates the growth and anti-ferroptosis of gastric cancer cells and predicts poor prognosis of gastric cancer. Aging. 2020;12(15):15374–91.
26. Lai Y, Zhang Z, Li J, Li W, Huang Z, Zhang C, Li X, Zhao J. STYK1/NOK correlates with ferroptosis in non-small cell lung carcinoma. Biochem Biophys Res Commun. 2019;519(4):659–66.

27. McCarthy DJ, Chen Y, Smyth GK. Differential expression analysis of multifactor RNA-Seq experiments with respect to biological variation. Nucleic Acids Res. 2012;40(10):4288–97.
28. Robinson MD, McCarthy DJ, Smyth GK. edgeR: a Bioconductor package for differential expression analysis of digital gene expression data. Bioinformatics. 2010;26(1):139–40.
29. Ritchie ME, Phipson B, Wu D, Hu Y, Law CW, Shi W, Smyth GK. limma powers differential expression analyses for RNA-sequencing and microarray studies. Nucleic Acids Res. 2015;43(7):e47.
30. Heagerty PJ, Lumley T, Pepe MS. Time-dependent ROC curves for censored survival data and a diagnostic marker. Biometrics. 2000;56(2):337–44.
31. Yu G, Wang LG, Han Y, He QY. clusterProfiler: an R package for comparing biological themes among gene clusters. Omics. 2012;16(5):284–7.
32. Hänzelmann S, Castelo R, Guinney J. GSVA: gene set variation analysis for microarray and RNA-seq data. BMC Bioinformatics. 2013;14:7.
33. Newman AM, Liu CL, Green MR, Gentles AJ, Feng W, Xu Y, Hoang CD, Diehn M, Alizadeh AA. Robust enumeration of cell subsets from tissue expression profiles. Nat Methods. 2015;12(5):453–7.
34. Brent RSPFA, Hülya B, Bush AI, Conrad M, Dixon S, Fulda S, Gascon S, Stavroula K, Hatzios V, Kagan K, Noel X, Jiang A, Linkermann ME, Murphy, Michael Overholtzer, Atsushi Oyagi, Gabriela Pagnussat, Jason Park, Qitao Ran, CS, Rosenfeld, Konstantin Salnikow, Daolin Tang, Frank Torti, Suzy Torti, Shinya Toyokuni, KA, Woerpel. and Donna D. Zhang: **Ferroptosis**: **a regulated cell death nexus linking metabolism**, **redox biology**, **and disease**. *Cell* 2017 October 05, **171**(**2**):**273**–**285**.
35. Ishii T, Warabi E, Mann GE. Circadian control of BDNF-mediated Nrf2 activation in astrocytes protects dopaminergic neurons from ferroptosis. Free Radic Biol Med. 2019;133:169–78.
36. Kang R, Kroemer G, Tang D. The tumor suppressor protein p53 and the ferroptosis network. Free Radic Biol Med. 2019;133:162–8.
37. Luo M, Wu L, Zhang K, Wang H, Zhang T, Gutierrez L, O'Connell D, Zhang P, Li Y, Gao T, et al. miR-137 regulates ferroptosis by targeting glutamine transporter SLC1A5 in melanoma. Cell Death Differ. 2018;25(8):1457–72.
38. Saint-Germain E, Mignacca L, Vernier M, Bobbala D, Ilangumaran S, Ferbeyre G: **SOCS1 regulates senescence and ferroptosis by modulating the expression of p53 target genes**. *Aging (Albany NY)* 2017, **9**(10):2137–2162.
39. Su L, Jiang X, Yang C, Zhang J, Chen B, Li Y, Yao S, Xie Q, Gomez H, Murugan R, et al. Pannexin 1 mediates ferroptosis that contributes to renal ischemia/reperfusion injury. J Biol Chem. 2019;294(50):19395–404.
40. Sun X, Ou Z, Xie M, Kang R, Fan Y, Niu X, Wang H, Cao L, Tang D. HSPB1 as a novel regulator of ferroptotic cancer cell death. Oncogene. 2015;34(45):5617–25.
41. Zhang X, Du L, Qiao Y, Zhang X, Zheng W, Wu Q, Chen Y, Zhu G, Liu Y, Bian Z, et al. Ferroptosis is governed by differential regulation of transcription in liver cancer. Redox Biol. 2019;24:101211.
42. Dixon SJ, Lemberg KM, Lamprecht MR, Skouta R, Zaitsev EM, Gleason CE, Patel DN, Bauer AJ, Cantley AM, Yang WS, et al. Ferroptosis: an iron-dependent form of nonapoptotic cell death. Cell. 2012;149(5):1060–72.
43. Jiang X, Stockwell BR, Conrad M. Ferroptosis: mechanisms, biology and role in disease. Nat Rev Mol Cell Biol. 2021;22(4):266–82.
44. Molinaro AM, Taylor JW, Wiencke JK, Wrensch MR. Genetic and molecular epidemiology of adult diffuse glioma. Nat Rev Neurol. 2019;15(7):405–17.
45. Reifenberger G, Wirsching HG, Knobbe-Thomsen CB, Weller M. Advances in the molecular genetics of gliomas - implications for classification and therapy. Nat Rev Clin Oncol. 2017;14(7):434–52.
46. Sarikonda G, von Herrath MG. Immunosuppressive mechanisms during viral infectious diseases. Methods Mol Biol. 2011;677:431–47.

47. Jaworski FM, Gentilini LD, Gueron G, Meiss RP, Ortiz EG, Berguer PM, Ahmed A, Navone N, Rabinovich GA, Compagno D, et al. In Vivo Hemin Conditioning Targets the Vascular and Immunologic Compartments and Restrains Prostate Tumor Development. Clin Cancer Res. 2017;23(17):5135–48.
48. Baxter RC. IGF binding proteins in cancer: mechanistic and clinical insights. Nat Rev Cancer. 2014;14(5):329–41.
49. Wang B, Rong X, Palladino END, Wang J, Fogelman AM, Martín MG, Alrefai WA, Ford DA, Tontonoz P. Phospholipid Remodeling and Cholesterol Availability Regulate Intestinal Stemness and Tumorigenesis. Cell Stem Cell. 2018;22(2):206–20.e204.
50. Gimple RC, Kidwell RL, Kim LJY, Sun T, Gromovsky AD, Wu Q, Wolf M, Lv D, Bhargava S, Jiang L, et al. Glioma Stem Cell-Specific Superenhancer Promotes Polyunsaturated Fatty-Acid Synthesis to Support EGFR Signaling. Cancer Discov. 2019;9(9):1248–67.
51. Bi J, Chowdhry S, Wu S, Zhang W, Masui K, Mischel PS. Altered cellular metabolism in gliomas - an emerging landscape of actionable co-dependency targets. Nat Rev Cancer. 2020;20(1):57–70.

Tables

Table 1

The clinical and molecular characteristic of samples in GTEx, TCGA, CGGA, Gravendeel and REMBRANDT

	GTEx	TCGA	CGGA	Gravendeel	REMBRANDT
Number of patients	105	687	693	276	383
Age					
< 60y		520	609	197	
≥ 60y		155	83	79	
Gender					
Female	32	286	295	92	121
Male	73	392	398	184	203
Grade					
I				8	2
II		251	188	24	92
III		260	255	85	70
IV		165	249	159	181
IDH1 Status					
Wildtype		398	286	140	
Mutation		276	356	81	
1p19q Codeletion					
Codeletion		169	145	47	24
Non-codeletion		485	478	85	150
MGMTmethylation					
Methylated		472	315		
Unmethylated		157	227		

Table 2

Result of univariate Cox regression analysis of ferroptosis-related genes

Genes	Beta	HR(95%CI)	z pvalue	Wald pvalue	Likelihood pvalue
ACSF2	0.33	1.39(1.20-1.62)	1.79E-05	1.79E-05	9.83E-06
ACSL4	-0.499	0.61(0.50-0.74)	7.34E-07	7.34E-07	1.18E-06
ALDH1L2	-0.566	0.57(0.51-0.63)	5.56E-26	5.56E-26	1.96E-24
ATP5G3	0.715	2.05(1.71-2.44)	3.36E-15	3.36E-15	1.21E-13
CISD1	-0.924	0.40(0.32-0.49)	4.54E-19	4.54E-19	7.30E-18
CS	-1.054	0.35(0.25-0.49)	8.82E-10	8.82E-10	2.44E-09
DDIT3	0.422	1.53(1.38-1.69)	4.20E-16	4.20E-16	8.67E-13
DPP4	0.382	1.47(1.39-1.55)	3.68E-42	3.68E-42	4.32E-35
ELAVL1	0.693	2.00(1.30-3.08)	1.63E-03	1.63E-03	1.98E-03
FANCD2	0.622	1.86(1.68-2.06)	1.10E-32	1.10E-32	6.37E-31
GCLM	0.921	2.51(2.14-2.95)	9.76E-29	9.76E-29	7.92E-26
GPX4	0.441	1.56(1.22-1.98)	3.04E-04	3.04E-04	4.78E-04
HMGB1	-0.660	0.52(0.37-0.73)	2.08E-04	2.08E-04	2.51E-04
HMOX1	0.549	1.73(1.59-1.89)	1.82E-35	1.82E-35	1.28E-32
IGFBP3	0.412	1.51(1.41-1.62)	1.04E-32	1.04E-32	4.14E-34
LONP1	-0.631	0.53(0.40-0.70)	7.77E-06	7.77E-06	1.94E-05
LPCAT3	0.635	1.89(1.63-2.19)	2.90E-17	2.90E-17	2.65E-14
LRP1	-0.332	0.72(0.60-0.86)	2.64E-04	2.64E-04	4.13E-04
NCOA4	-1.331	0.26(0.21-0.33)	1.13E-32	1.13E-32	1.81E-29
NFE2L2	1.037	2.82(2.05-3.89)	2.42E-10	2.42E-10	7.24E-11
SAT1	0.770	2.16(1.92-2.43)	7.85E-38	7.85E-38	1.65E-32
SLC40A1	0.441	1.56(1.38-1.76)	1.74E-12	1.74E-12	4.08E-12
SLC7A11	-0.258	0.77(0.69-0.87)	1.81E-05	1.81E-05	2.28E-05
TF	-0.237	0.79(0.74-0.84)	8.21E-13	8.21E-13	1.12E-11
TFRC	0.830	2.28(2.02-2.58)	5.91E-40	5.91E-40	5.73E-38
TP53	0.490	1.63(1.38-1.93)	9.51E-09	9.51E-09	2.34E-09

Table 3

Baseline characteristics of the patients in different risk groups

Variables	TCGA			CCGA			Gravendeel			REMBRANDT		
										Gravendeel		
	High risk	Low risk	P value	High risk	Low risk	P value	High risk	Low risk	P value	High risk	Low risk	P value
Age			<0.001			0.005			<0.001			
< 60y	150	372		289	320		88	109				
≥ 60y	99	56		53	30		58	21				
unknown	2	8		1	0		0	0				
Gender			0.195			0.757			0.67			0.422
Female	97	189		144	151		47	45		63	58	
Male	152	240		199	199		99	85		115	88	
unknown	2	7		0	0		0	0		39	20	
Grade			<0.001			<0.001			<0.001			<0.001
I	0	0		0	0		3	5		2	0	
II	17	234		43	145		3	21		23	69	
III	76	184		115	140		31	54		36	34	
IV	156	9		184	65		109	50		146	35	
unknown	2	9		1	0		0	0		10	28	
IDH1 Status			<0.001			<0.001			<0.001			
Wildtype	199	77		193	93		26	51				
Mutation	49	349		142	214		89	55				
unknown	3	10		8	43		31	24				
1p19q			<0.001			<0.001			<0.001			<0.001
Codeletion	7	162		40	105		10	37		4	20	
Non-codeletion	220	265		301	177		55	30		96	54	
unknown	24	9		2	68		81	63		117	92	
MGMT			<0.001			0.101						
Methylated	106	366		151	164							
Unmethylated	96	61		125	102							
unknown	49	9		67	84							

Table 4

Result of univariate cox analysis in TCGA, CGGA, REMBRANDT and Gravendeel datasets

	Univariate Cox	Beta	HR	z_ pvalue	Wald _pvalue	Likelihood P value
TCGA	Risk score	2.258	9.57(6.88-13.31)	0	0	0
	Grade	1.700	5.48(4.35-6.89)	0	0	0
	Gender	0.230	1.26(0.95-1.67)	0.116	0.116	0.112
	Age	1.631	5.11(3.86-6.76)	0	0	0
	IDH1 Status	-2.473	0.08(0.06-0.12)	0	0	0
	X1p19q codeletion	-1.764	0.17(0.1-0.31)	0	0	0
	MGMT methylation	-1.492	0.22(0.16-0.31)	0	0	0
	Histology	1.061	2.89(2.44-3.43)	0	0	0
CGGA	Risk score	1.175	3.24(2.62-4.00)	0	0	0
	Grade	0.981	2.67(2.30-3.09)	0	0	0
	Gender	0.059	1.06(0.87-1.30)	0.563	0.563	0.563
	IDH1 Status	-1.129	0.32(0.26-0.40)	0	0	0
	X1p19q codeletion	-1.317	0.27(0.19-0.37)	0	0	0
	Age	0.830	2.29(1.76-2.98)	0	0	0
	MGMT methylation	-0.229	0.80(0.64-0.99)	0.041	0.041	0.041
	Histology	0.157	1.17(1.14-1.20)	0	0	0
	PRS type	0.780	0.27(1.79-2.67)	0	0	0
Gravendeel	Risk score	1.156	2.92(2.19-3.88)	0	0	0
	Gender	0.074	1.08(0.79-1.46)	0.637	0.637	0.635
	Grade	1.0706	3.18(2.33-4.34)	0	0	0
	IDH1 status	-0.986	0.37(0.26-0.54)	0	0	0
REMBRANDT	Risk score	1.031	2.80(2.1-3.75)	0	0	0
	Grade	0.661	1.94(1.62-2.32)	0	0	0

Figures

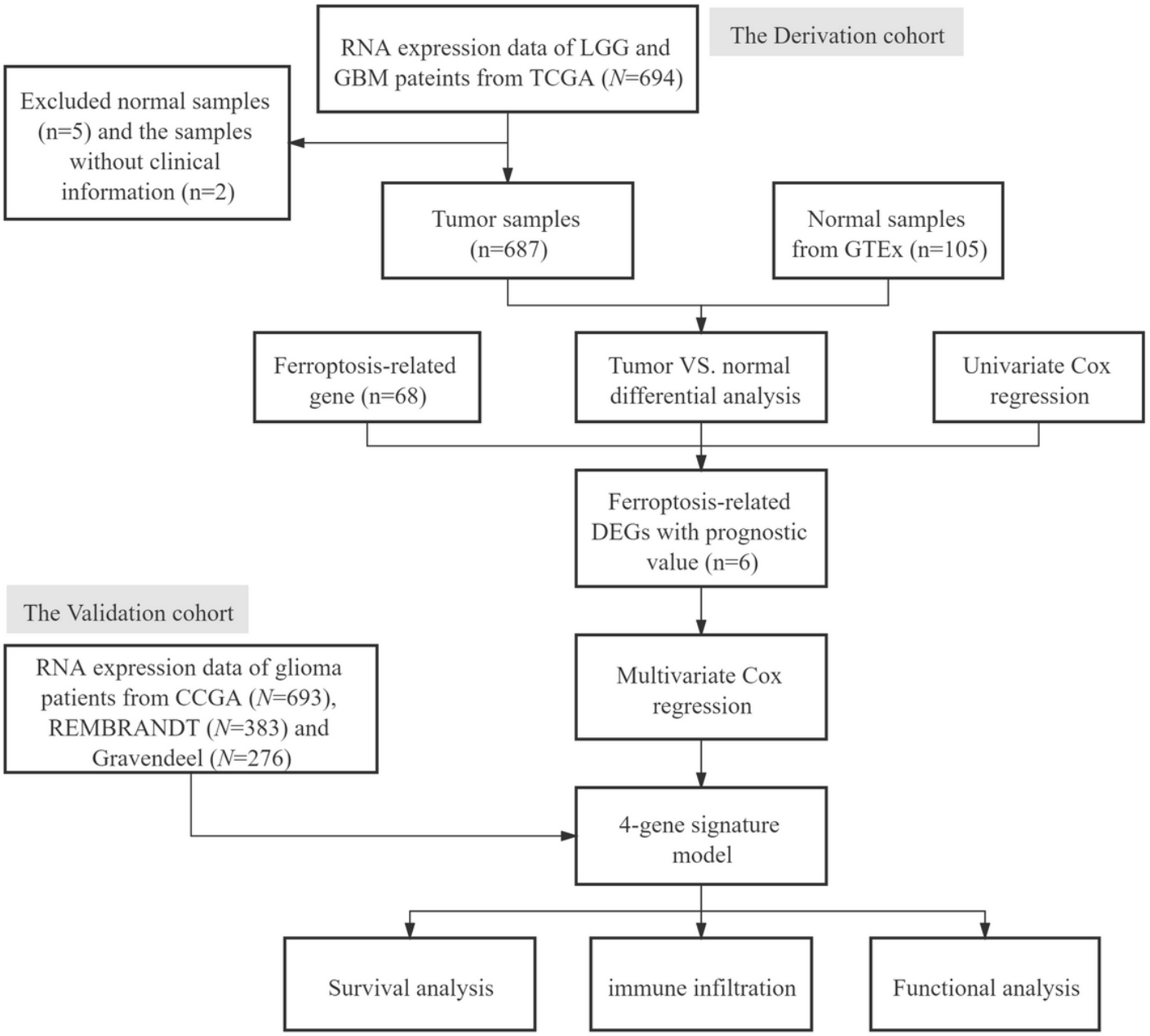

Figure 1

Flow chart of data collection and gene model generation and validation procedures.

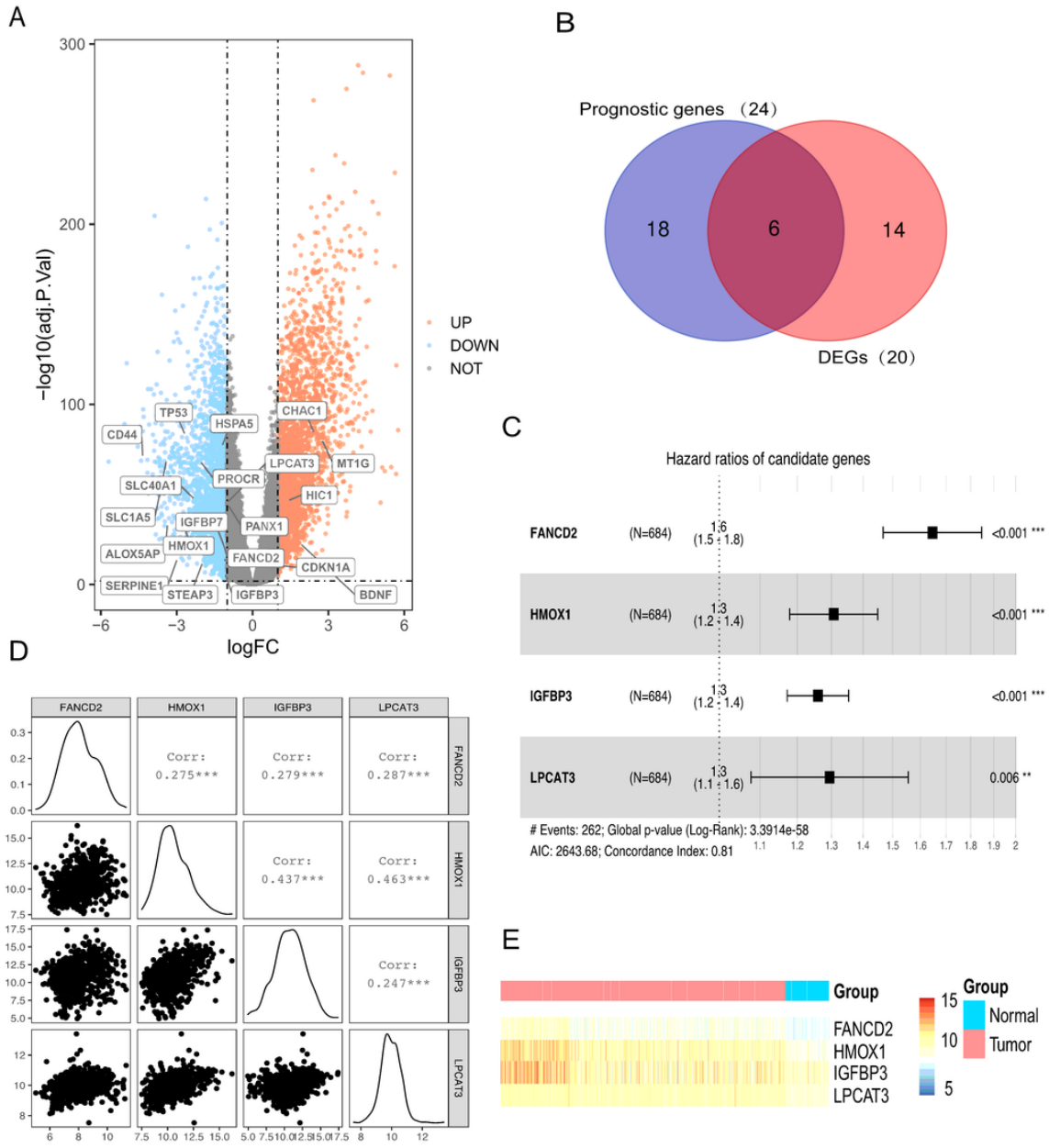

Figure 2

Identification of 4 ferroptosis-related candidate genes in TCGA cohort. A. The volcano figure shows the differential expression of 23 ferroptosis-related genes in 4352 DEGs between normal and tumor tissues. B. Venn diagram to identify differentially expressed ferroptosis-related genes that were correlated with OS. C. Forest plot shows the coefficient of the 6 genes. TP53 and SLC40A1 were not significant. D. The correlation plot shows the co-linearity between the 4 genes. E. The heatmap shows the expression of 4 genes in normal and glioma tissues.

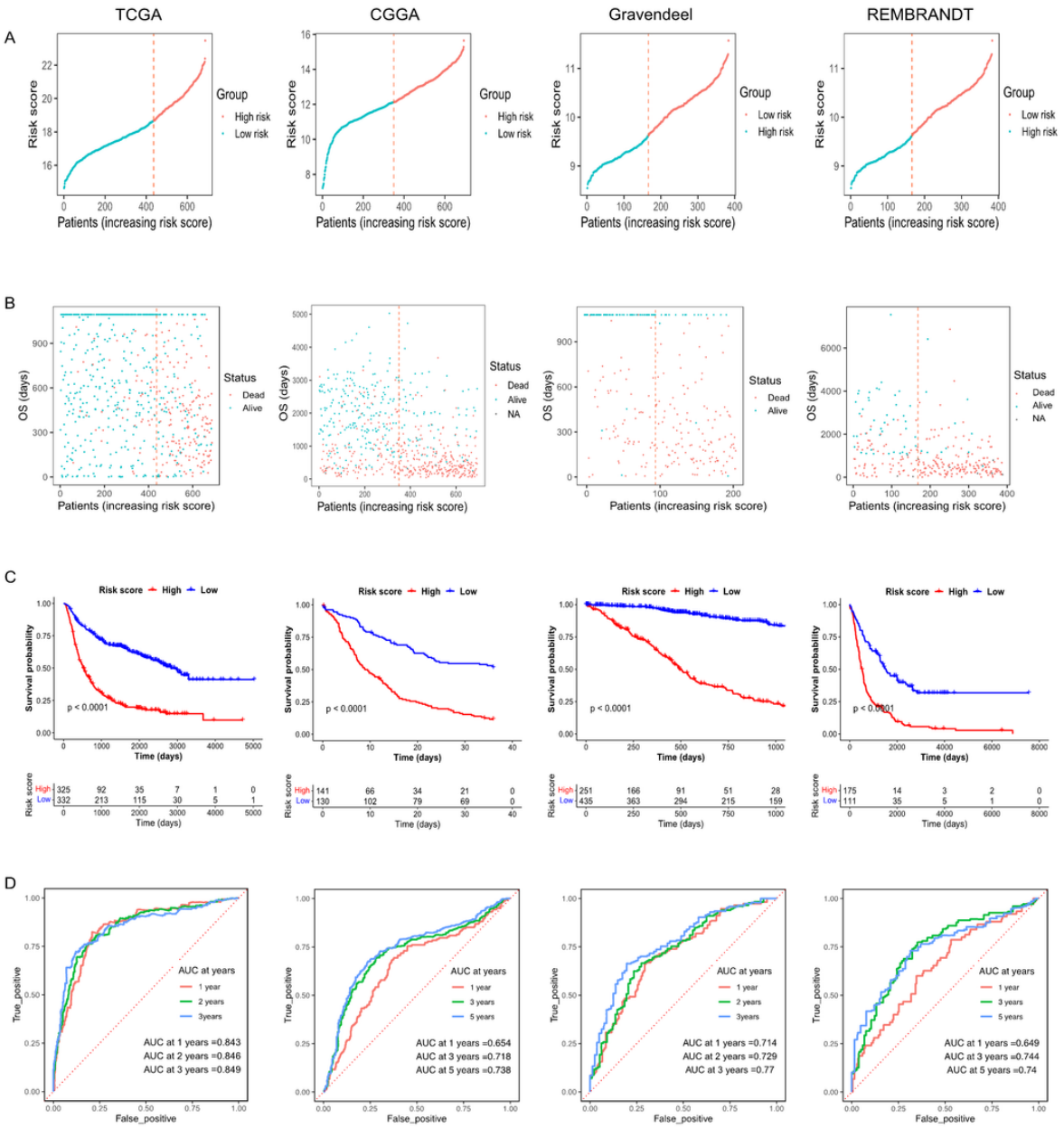

Figure 3

Distribution of risk score and OS and Kaplan-Meier survival analysis in TCGA, CGGA, Gravendeel and REMBRANDT datasets. A. Patients' risk score distribution in four datasets. B. The distribution of OS and OS status in four datasets. C. Kaplan-Meier curves for glioma patients of low and high-risk scores in four datasets.

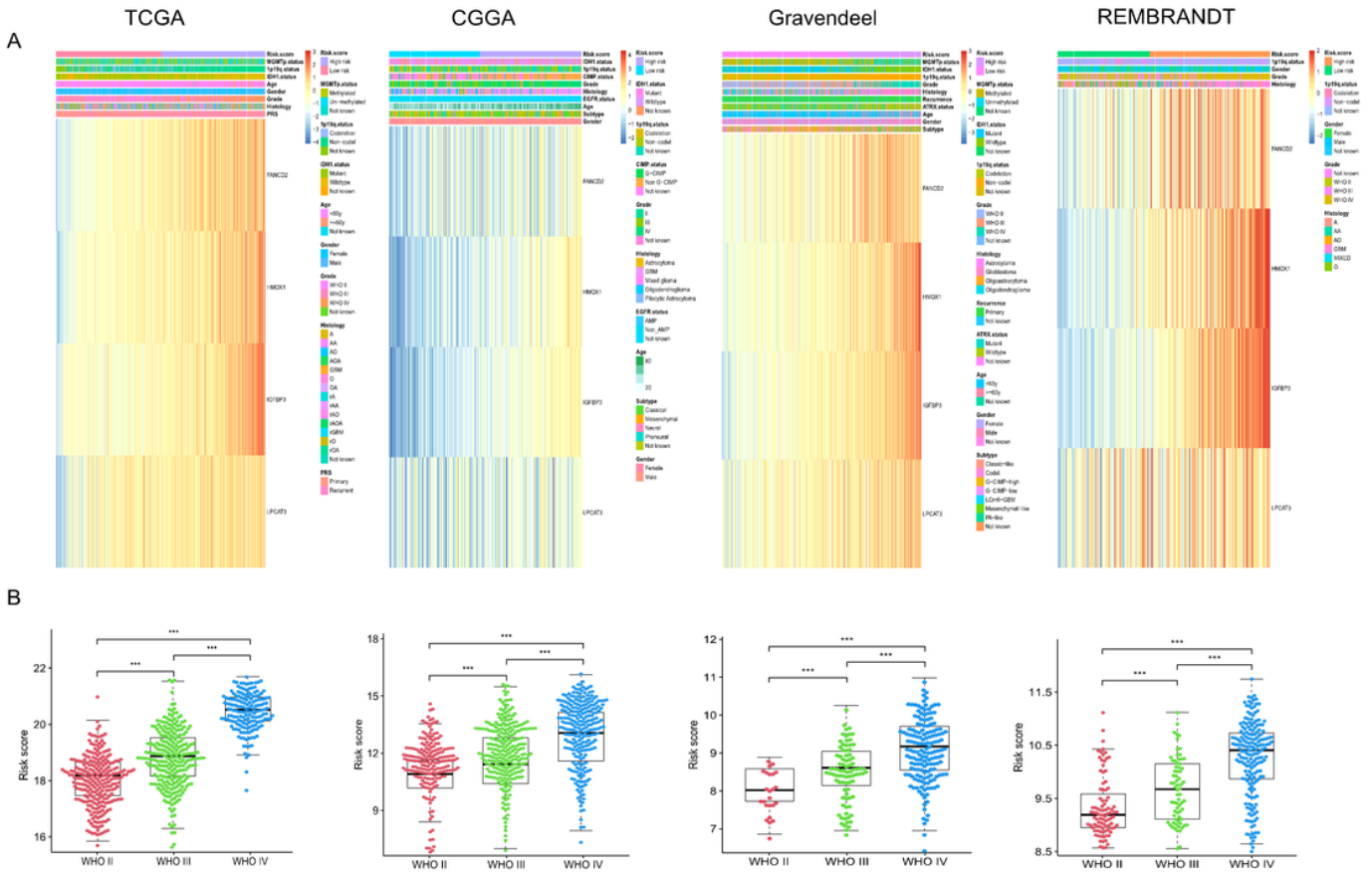

Figure 4

Ferroptosis-related prognosis genes expression profiles and Risk score of WHO grade subgroups in TCGA, CGGA, Gravendeel and REMBRANDT datasets. A. Heatmaps show the different expression levels of 4 ferroptosis-related prognosis genes and their correlation between signature risk score, clinical and molecular pathological features in four datasets. B. Risk score value in different WHO grade subgroup in four datasets.

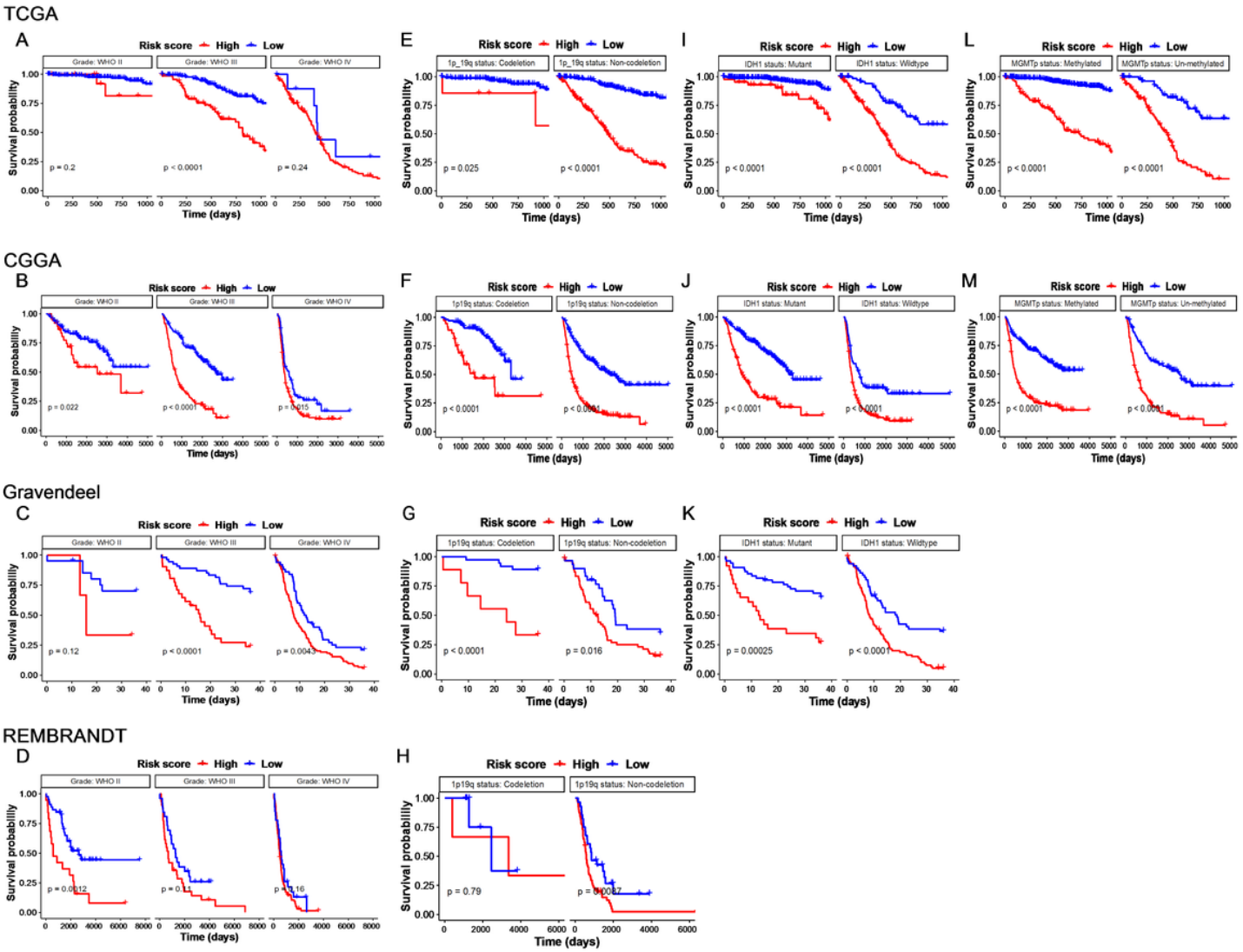

Figure 5

Survival analyses of the 4-genes model based on four databases (TCGA, CGGA, Gravendeel and REMBRANDT) with clinical characters (WHO grade, IDH1, MGMT, 1p/19q) subgroups. A. TCGA. B. CGGA. C. Gravendeel. D. REMBRANDT.

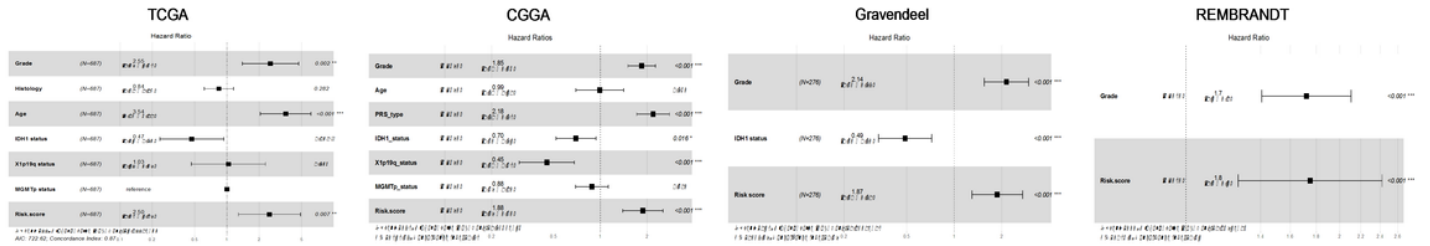

Figure 6

The result of multivariate Cox regression analysis regarding OS in TCGA, CGGA, Gravendeel and REMBRANDT datasets. A. TCGA. B. CGGA. C. Gravendeel. D. REMBRANDT.

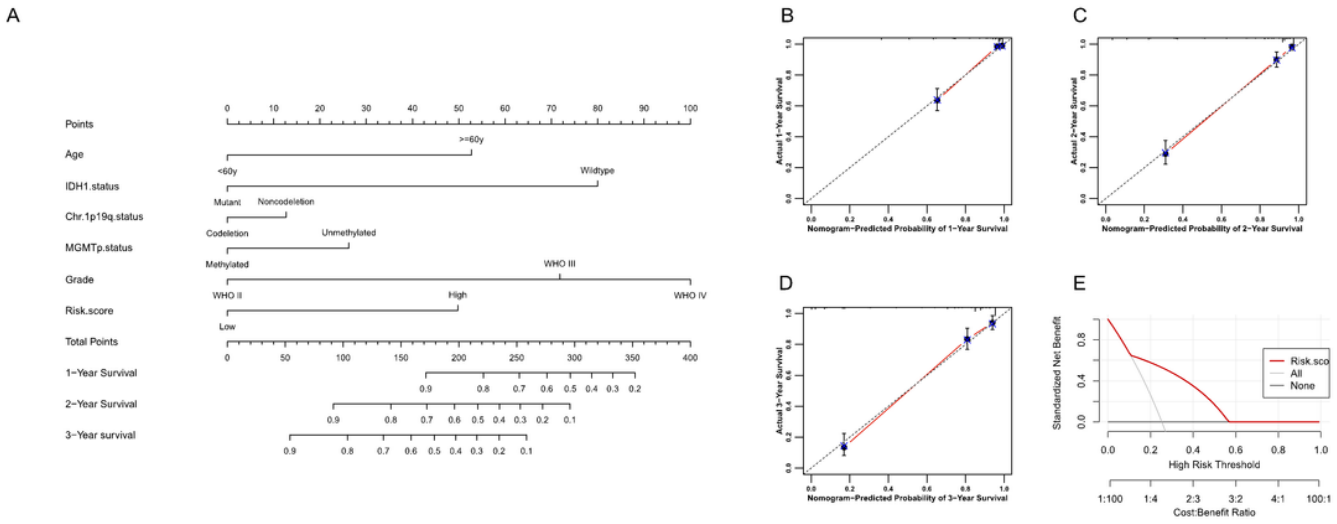

Figure 7

Nomogram for predicting ferroptosis-gene-model clinical value, calibration of the nomogram OS and decision curve in the overall patients. A. Nomogram for predicting ferroptosis-genes model clinical value (B-D). Calibration curves in the 1-year, 2-year, and 3-year Survival. E. decision curve in the overall patients.

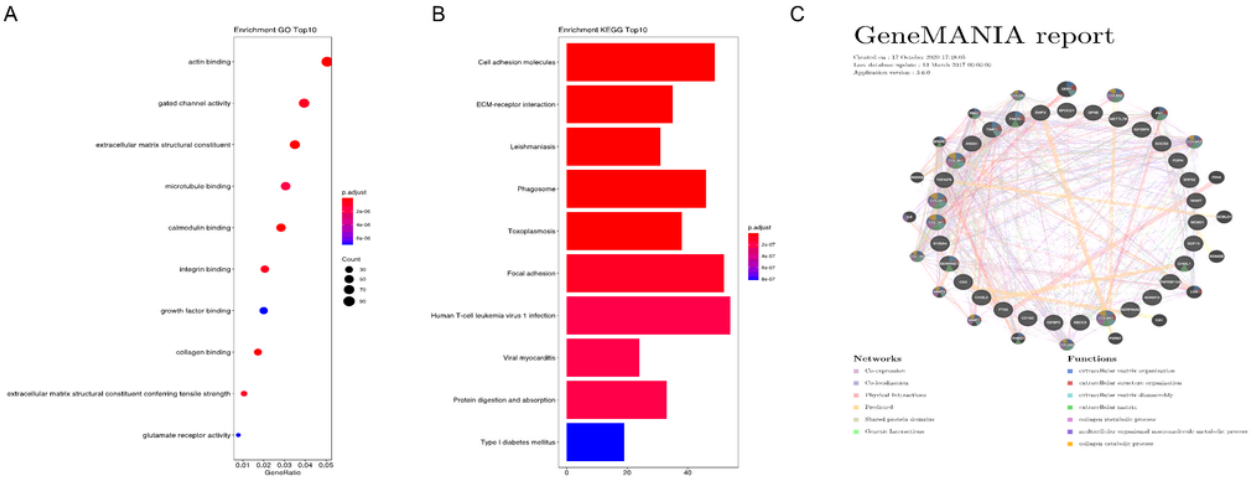

Figure 8

Representation results of GO and KEGG analysis and the result of GeneMANIA. A. The most significant GO enrichment in TCGA dataset. B. The most significant KEGG pathways in TCGA dataset. C. The result of GeneMANIA based on DEGs between low-risk and high-risk groups in TCGA dataset.

Pathway	TCGA PVaue	CGGA PVaue	Gravendeel PVaue	REMBRANDT PVaue
Epithelial Mesenchymal Transition	<0.001	<0.001	<0.001	<0.001
IL6 JAK STAT3 signaling	<0.001	<0.001	<0.001	<0.001
Interferon gamma response	<0.001	<0.001	<0.001	<0.001
IL2 STAT5 signaling	<0.001	<0.001	<0.001	<0.001
TNFA signaling via NFKB	<0.001	<0.001	<0.001	<0.001
Interferon alpha response	<0.001	<0.001	<0.001	<0.001
Glycolysis	<0.001	<0.001	<0.001	<0.001

Figure 9

Gene-set variation analysis and Immune infiltration. (A-D). Differences in pathway activities scored by GSVA between high- and low-risk patients in four databases. T values are shown from a linear model. Half of the maximum value of each calculation is taken as the cutoff value. The blue column indicates activated pathways in high-risk patients, and the green column indicates activated pathways in low-risk patients (DN, down; UV, ultraviolet; v1, version 1; v2, version 2). (E-F). Venn diagram shows intersection-based of four databases pathway activited. Table presents the specific pathways. (G-H). The infiltration of immune cells in two databases (TCGA and CGGA) based on Cibersort.

Supplementary Files

This is a list of supplementary files associated with this preprint. Click to download.

- Supplement.docx